

# Coding strategies for static patterns suitable for UV deflectometry

## Codierungsstrategien für in der UV-Deflektometrie anwendbare Muster

Christian Kludt<sup>1</sup> and Jan Burke<sup>2</sup>

<sup>1</sup> Karlsruhe Institute of Technology,  
Karlsruhe School of Optics and Photonics,  
Kaiserstraße 12, 76131 Karlsruhe

<sup>2</sup> Fraunhofer IOSB,  
Fraunhoferstraße 1, 76131 Karlsruhe

**Abstract** We introduce a method based on the deflectometry principle for the inspection of transparent, rotation-symmetric objects with steep angles. Examples are intraocular or strongly curved, aspheric lenses. Usually, an additional reflection at the lens' back side occurs and disturbs the signal. The solution is to use ultraviolet light which does not penetrate the material. As a consequence, static masks have to be used to generate the fringe pattern. A key feature of our approach is the specification of a spiral pattern, that meets the requirements for ultraviolet deflectometry with static masks. The spiral patterns are decoded by a multi-frequency phase shifting algorithm. We explain the principles of pattern design and present first evaluation results. Furthermore, we introduce a straight forward approach to obtain the absolute coordinates of the screen directly without any unwrapping. This facilitates the reconstruction of the three-dimensional shape of the lens in a subsequent step.

**Keywords** Optical Inspection, Lens Testing, Deflectometry, Fringe Analysis, Phase Measurement.

## 1 Introduction

In some medium-uncertainty applications, interferometry can today be replaced by phase measuring deflectometry (PMD) as a tool for

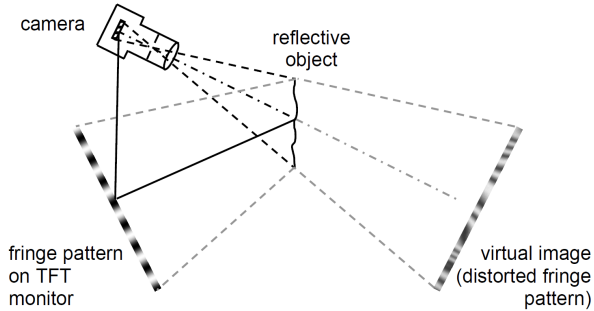


**Figure 1:** Deflectometry setup. A regular fringe pattern is displayed on a monitor, gets reflected and distorted by the object and is captured by the camera. From [3].

lens inspection [1], [2]. Deflectometric sensors provide often sufficient accuracy and benefit from their cost-effective components that consist only of a monitor and a camera. The monitor displays a regular reference pattern that is reflected by the object's surface and captured by the camera. If the object's surface shows topographic irregularities such as dents and bumps, the recorded pattern appears distorted. By analyzing the deformation and displacement compared to the reference pattern, and having a calibrated system, i.e. knowing the position and orientation of both monitor and camera, it is also possible to reconstruct the global surface shape. The basic setup is shown in Figure 1.

However, when inspecting transparent objects, one will observe an additional reflection from the object's back side. It is superimposed onto the front side reflection, generating an unwanted extra signal that cannot be processed by conventional evaluation procedures [4] and at some locations cannot be analyzed at all [5].

## 2 Existing approaches

A suitable solution is to apply light at a spectral range where the object's material is non-transparent. Most organic lenses are made from polymethyl methacrylate (PMMA), which is blended to be absorbing

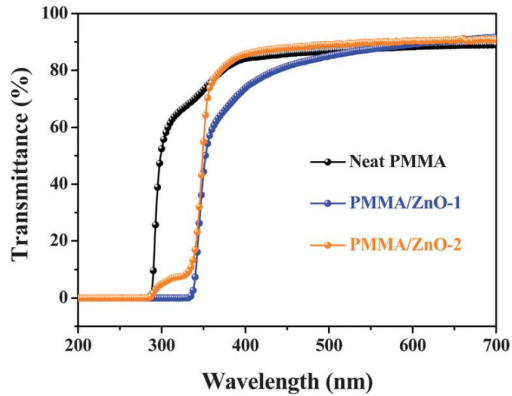


**Figure 2:** Transmission spectra of pure and blended PMMA. From [6].

for ultraviolet (UV) radiation [6]. Figure 2 shows the transmission spectra of pure and blended PMMA. Consequently, in the UV the reflection takes place only at its front side.

**Problem 1:** There is no spatial pattern generator available working in the UV range, as there is in the visual range (e.g. TFT monitors or OLED panels). So one key issue is how to generate the reference fringe pattern at the appropriate wavelength.

**Problem 2:** Fringe compression occurs at objects with steep edges or strongly curved surfaces. This is due to perspective shortening effects from the camera's line of sight and widening of its sight ray when reflected at convex surfaces. In Figure 3(b) this effect occurs at the periphery of a lens. In the area marked red, the fringes of the reflected pattern become very dense and eventually cannot be resolved anymore.

**Solution to 1:** Sprenger et al. [9] illuminate a slit mask with a UV light source to create a UV line lighting. However, the downside of this approach is its only one-dimensional extent. To acquire the second

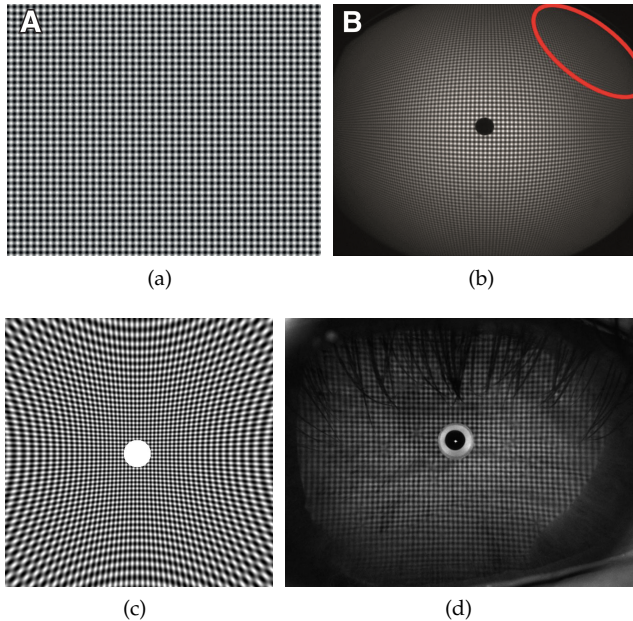


**Figure 3:** (a) Preditorted Cartesian fringe pattern. (b) Straight fringe pattern reflected from cornea. (c) Reference pattern with straight fringes. (d) Reflected reference pattern shows fringe compression at the edging of a lens. From [7], [8].

dimension, a time consuming scanning process is required to compile an image of the whole object covered by fringes. A straight forward approach is to create a metallic pattern and illuminate it with ultraviolet light or to place a two-dimensional mask transmissive in the UV in front of a UV light source. In any case, it will be a static pattern and hence has to be moved mechanically if phase shifting techniques are applied.

**Solution to 2:** Fringe compression by convex lenses can be compensated by using predistorted reference patterns that are matched to their rotational symmetry. Figure 3(c) shows a predistorted Cartesian

fringe pattern that compensates the distortion caused by the cornea of a human eye. As a result, the reflected pattern shows straight fringes and uniform fringe spacing, cf. Figure 3(d). This ensures constant fringe resolution throughout the image plane.

But temporal phase shifting (TPS) [10] is difficult with current predistorted, static patterns: As predistortion introduces a non-uniform scale, each point will be shifted by a different fraction of periods when the pattern is moved. So, if each point of the pattern is to be shifted by the same fraction of periods, they each have to be moved by a different distance or corrections for non-uniform phase shifts must be used. Hence, the pattern does not coincide with itself after shifting, and instead behaves like a dynamic pattern.

While solutions already exist for the individual problems, there still is no solution to the combined problem: There is no spatial light modulator available in the UV range that provides predistortion for convex, rotation symmetric objects (such as lenses) and stays congruent when it is shifted.

### 3 Proposed method

In order to obtain two phase maps with an orthonormal basis, modulation must be applied to a fringe pattern in two linearly independent directions. The basic approach is to shift a sinusoidal fringe pattern laterally in one direction, then rotate it by 90 degrees and shift it again. This requires  $N$  phase shifts per direction, so a total number of  $2N$  phase shifts is required.

A more efficient method is demonstrated by Liu et al. [11]: A one-dimensional phase shift is applied to a crossed fringe pattern. The phase shifting direction must not be parallel to any of the fringes so as to create simultaneous phase modulation of both fringe orientations. At this, each point is shifted by a different integer number of periods for the  $x$  and  $y$  direction, respectively. In Figure 4, a red marker is drawn at a fixed phase to visualize the pattern translation. To decode the phase information, the phase shifting algorithm (PSA) is adjusted

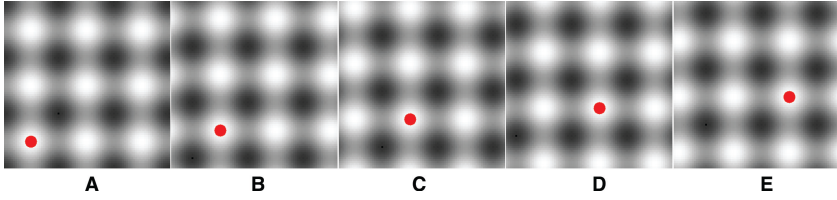


**Figure 4:** One-dimensional phase shift by two periods horizontally and one period vertically. From [11].

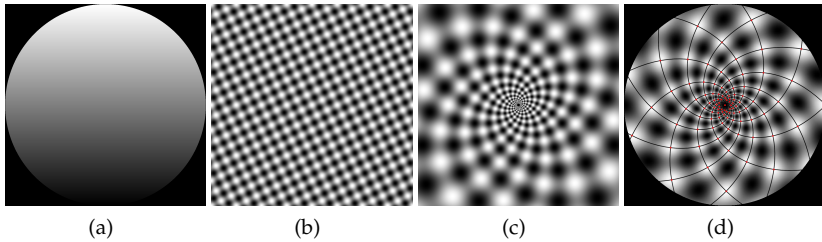


**Figure 5:** (a) Linear gray scale pattern. (b) Cartesian coordinate system with regular, straight fringes. (c) Log-polar coordinate system with spiral fringes. (d) Intersections of spiral arms, indicated as red dots. They provide an orthonormal basis in each point.

to the number of shifted periods, i.e. it is made frequency-selective. This corresponds to applying the discrete Fourier transform (DFT) to the phase shifting sequence and reduces the number of exposures to  $N$ .

An alternative approach is encoding the screen not by a cosine pattern but by a linear gray scale [12], cf. Figure 5(a). It is rotated around its center and due to its width predistortion is not required. For phase decoding, only  $N = 3$  phase shifts are needed.

Ziebarth et al. [13] introduced a novel pattern design based on spinning spirals. It exploits the rotational symmetry of lenses and enables TPS techniques to be applied to predistorted, static patterns. Instead of Cartesian coordinates as in Figure 5(b), fringe patterns are generated in Log-polar coordinates, see Figure 5(c). The final crossed fringe pattern

depicted in Figure 5(d) is the superposition of two counter rotating spiral patterns. Phase shifting is not applied in lateral but in angular direction, i.e. the spirals are spinning around their center, therefore the name.

Crossed fringe patterns with logarithmic spirals offer the following characteristics:

- During rotation, the modulation in both spiral directions is achieved, which enables phase decoding in two linearly independent directions.
- They are rotationally symmetric and therefore coincide with themselves after being rotated by certain angles, i.e. the rotation is a congruence mapping. This allows for the use of static, mechanically moved patterns.
- A special property of logarithmic spirals is their constant slope and therefore intersection angle with the tangential and radial line. Hence, the spiral crossed fringe pattern has an orthonormal basis at each point, see the crossing points in Figure 5(d). This simplifies the calculation of the surface slope in a subsequent step.
- A substantial feature is their inherent predistortion: The width of the spiral arms increases with the radius, thereby compensating the fringe compression by strong positive lenses. Of course the opposite effect occurs when moving along the spirals to their origin. In the center, the fringes become too dense to be resolved by the camera. In practice, however, the camera will be placed here anyway, as in Figure 3(d).

## 4 Coding scheme

In conventional TPS in the visual range, each pattern is displayed and shifted separately. Since in the UV static masks have to be used, the individual patterns have to be superimposed to create a composite, crossed fringe pattern. In order to extract the contained patterns, we propose a *multi-frequency phase coding* technique.

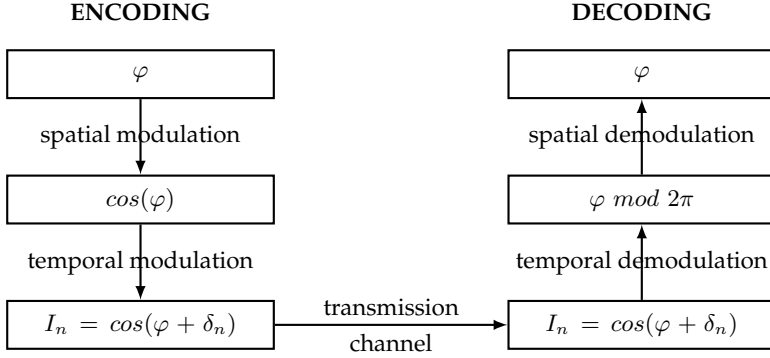


**Figure 6:** Signal model of a deflectometric coding scheme.

To understand the individual steps, its signal model is depicted in Figure 6. The screen coordinates are represented by the phases  $\varphi_x$  and  $\varphi_y$  and in polar coordinates by  $\varphi_r$  and  $\varphi_\phi$ , respectively. For the sake of brevity we omit the location dependency and describe the coding scheme by the generic phase coordinate  $\varphi$ . To exploit the precision of phase shifting techniques, we introduce spatial modulation in the form of a cosine pattern. Now we apply TPS as we shift the pattern by the nominal phase increment  $\delta_n$  and receive the phase shifting sequence  $I_n$ , which is displayed on the monitor. The reflection from the object is modeled as the transmission channel of the system and is affected by additional noise [14], but in the following we assume an ideal channel. The camera's irradiance readings are temporally demodulated by PSAs into the wrapped phase distribution  $\varphi \bmod 2\pi$ . Spatial demodulation is achieved by unwrapping algorithms. Finally, the absolute phase  $\varphi$  is obtained, which identifies the screen coordinate, where the light impinging on each camera pixel originated from.

The crucial task is the stable algorithmic separation of the two superimposed fringe patterns from the composite pattern displayed in Figure 5(d). Each pattern contains a different number of spiral arms  $f$ , hence we can adjust our algorithm to each number and construct a frequency selective PSA. For this purpose, we apply the DFT algorithm to the phase shifting sequence  $I_n$  and extract the phases at the defined

frequencies. For this to function best, the pattern has to be shifted by one full revolution and a minimum number of  $N = 2f_{max} + 1$  incremental phase shifts is required. The results are the wrapped, but orthonormal phase distributions in Figure 7(a) and 7(b) that are only unambiguous within one fringe period. This is due to the  $2\pi$ -periodicity of the trigonometric functions within the PSA.

The absolute phase can be spatially unwrapped by analyzing neighbouring pixels [15], [16]. This will work fine on optical, but not flawlessly at discontinuous surfaces. For proper unwrapping, additional information is required. Therefore, a total of four patterns are required, with always two of them forming parallel pairs [12]. If the number of spirals within such a pair are primes, e.g.  $f_1 = 5$  and  $f_2 = 13$  spirals, the phase distribution can be unwrapped by applying the Chinese remainder theorem [17] and an absolute phase map is obtained.

Unwrapping is not required if we don't introduce spatial modulation at all. Hence, the temporal demodulation of the linear gray scale pattern yields the absolute screen coordinates directly. The DFT algorithm requires only  $N = 3$  phase shifts to compute at frequency  $f = 1$  the phase in Figure 7(c), which constitutes the angular coordinate  $\varphi_\phi$ . The radial coordinate  $\varphi_r$  in Figure 7(d) is obtained by computing the fringe modulation at the same frequency. This technique is more susceptible to noise because of its very low fringe frequency.

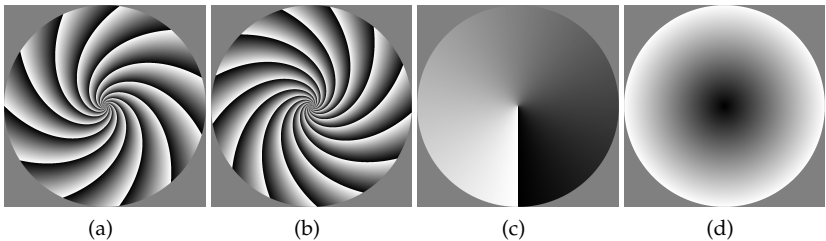


**Figure 7:** Phase Extraction. Temporal demodulation of the spiral pattern yields wrapped phases (a) and (b), whereas absolute phases (c) and (d) are obtained when the linear gray scale pattern is used.

## 5 Experiments

So far we assumed an error free transmission channel and simulated the decoding process, cf. Figure 7. To prove it to work in a real environment, we displayed the spiral crossed fringe pattern on a computer monitor and captured it directly with a camera. Although no reflecting object was in between and we were operating in the visual range, it resembles a deflectometric measurement as the setup adds noise to the signal. Figure 8(a) shows the rotated pattern. In Figure 8(b) and 8(c) the extracted, wrapped phases are depicted. The phase decoding works quite well and the technique appears stable under experimental conditions.

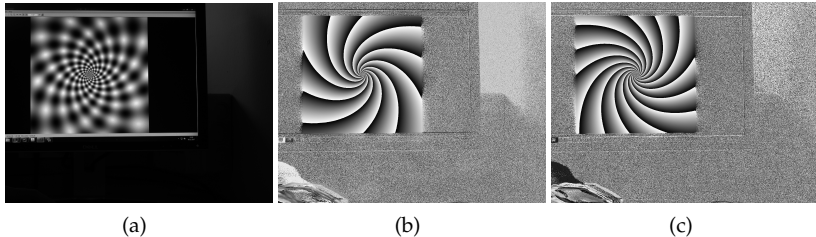


**Figure 8:** Deflectometric measurement. (a): Rotationally shifted spiral pattern. (b) and (c): Extracted phase maps.

## 6 Conclusion

We demonstrated the feasibility of spinning spirals, which allows for the use of static, but moving masks to extend the application of deflectometry outside the visual range. Their logarithmic scale compensates for fringe compression on strong convex lenses. The composite crossed fringe pattern is analyzed with the DFT algorithm, which extracts the phase maps at the prescribed frequencies. A simple but efficient approach utilizes a rotating gray scale and yields the absolute phase maps directly. Subject of current research is the reduction of the number  $N$  of phase shifts required to decode the phase shifting sequence appropriately on the basis of filters designed with Z-transform techniques [18].

## References

1. G. Häusler, "Verfahren und Vorrichtung zur Ermittlung der Form oder der Abbildungseigenschaften von spiegelnden oder transparenten Objekten," Germany Patent DE000 019 944 354B4, April, 1999. [Online]. Available: <https://register.dpma.de/DPMAregister/pat/PatSchrifteneinsicht?docId=DE19944354A1>
2. 3D-Shape GmbH. (2018) Optische Messtechnik für spiegelnde Oberflächen: SpecGAGE3D. <http://www.3d-shape.com/produkte/spiegelnde-oberflaechen.php>. 3D-Shape GmbH. [Online]. Available: [http://www.3d-shape.com/produkte/spiegelnde\\_oberflaechen.php](http://www.3d-shape.com/produkte/spiegelnde_oberflaechen.php)
3. P. Huke, J. Burke, and R. B. Bergmann, "A comparative study between deflectometry and shearography for detection of subsurface defects," pp. 9203 – 9203 – 12, 2014. [Online]. Available: <https://doi.org/10.1117/12.2063650>
4. C. Faber, M. C. Knauer, and G. Häusler, "Can deflectometry work in presence of parasitic reflections?" in *Proceedings of the 110<sup>th</sup> Annual DGaO Conference*, ser. DGaO Proceedings, vol. 110, DGaO, 2009, p. A10. [Online]. Available: <http://www.dgao-proceedings.de/download/110/110.a10.pdf>
5. C. Faber, E. Olesch, R. Krobot, and G. Häusler, "Deflectometry challenges interferometry: the competition gets tougher!" pp. 8493 – 8493 – 15, 2012. [Online]. Available: <https://doi.org/10.1117/12.957465>
6. Y. Zhang, X. Wang, Y. Liu, S. Song, and D. Liu, "Highly transparent bulk PMMA/ZnO nanocomposites with bright visible luminescence and efficient UV-shielding capability," *Journal of Materials Chemistry*, vol. 22, no. 24, p. 11971, 2012. [Online]. Available: <https://doi.org/10.1039/c2jm30672g>
7. H. Liang, E. Olesch, Z. Yang, and G. Häusler, "Single-shot phase-measuring deflectometry for cornea measurement," *Advanced Optical Technologies*, vol. 5, no. 5-6, pp. 1–6, jan 2016. [Online]. Available: <https://doi.org/10.1515%2Faot-2016-0049>
8. J. H. Massig, E. Lingelbach, and B. Lingelbach, "Videokeratoscope for accurate and detailed measurement of the cornea surface," *Appl. Opt.*, vol. 44, no. 12, pp. 2281–2287, 4 2005. [Online]. Available: <http://ao.osa.org/abstract.cfm?URI=ao-44-12-2281>
9. D. Sprenger, C. Faber, M. Seraphim, and G. Häusler, "Uv-deflectometry: No parasitic reflections," in *DGaO Proceedings*, vol. 111, 2010, p. A19.

10. H. Schreiber and J. H. Bruning, *Phase Shifting Interferometry*. Wiley-Blackwell, 2006, ch. 14, pp. 547–666. [Online]. Available: <https://onlinelibrary.wiley.com/doi/abs/10.1002/9780470135976.ch14>
11. Y. Liu, E. Olesch, Z. Yang, and G. Häusler, “Fast and accurate deflectometry with crossed fringes,” *Advanced Optical Technologies*, vol. 3, pp. 441–445, Aug. 2014.
12. C. Kludt, “Spinning Spirals - Measuring Optical Surfaces in Polar Coordinates,” Master’s Thesis, Karlsruhe Institute of Technology, 2018.
13. M. Ziebarth, T. Stephan, S. Höfer, and J. Burke, “Creating patterns for phase shifting by rotation in deflectometry,” in *DGao Proceedings*, vol. 118, 2017, p. B12. [Online]. Available: [http://www.dgao-proceedings.de/abstract/abstract\\_only.php?id=2194](http://www.dgao-proceedings.de/abstract/abstract_only.php?id=2194)
14. Y. Surrel, “Additive noise effect in digital phase detection,” *Appl. Opt.*, vol. 36, no. 1, pp. 271–276, Jan 1997. [Online]. Available: <http://ao.osa.org/abstract.cfm?URI=ao-36-1-271>
15. H. Lei, X. yu Chang, F. Wang, X.-T. Hu, and X.-D. Hu, “A novel algorithm based on histogram processing of reliability for two-dimensional phase unwrapping,” *Optik - International Journal for Light and Electron Optics*, vol. 126, no. 18, pp. 1640 – 1644, 2015. [Online]. Available: <http://www.sciencedirect.com/science/article/pii/S0030402615003228>
16. M. A. Herráez, D. R. Burton, M. J. Lalor, and M. A. Gdeisat, “Fast two-dimensional phase-unwrapping algorithm based on sorting by reliability following a noncontinuous path,” *Appl. Opt.*, vol. 41, no. 35, pp. 7437–7444, Dec 2002. [Online]. Available: <http://ao.osa.org/abstract.cfm?URI=ao-41-35-7437>
17. K. Ireland and M. Rosen, “The Chinese remainder theorem,” *A Classical Introduction to Modern Number Theory*, pp. 34–38, 1990.
18. Y. Surrel, “Design of algorithms for phase measurements by the use of phase stepping,” *Appl. Opt.*, vol. 35, no. 1, pp. 51–60, Jan 1996. [Online]. Available: <http://ao.osa.org/abstract.cfm?URI=ao-35-1-51>